Time-Resolved Study of Acetyl Radical in Zeolite NaY by Step-Scan FT-IR Spectroscopy

Sergey Vasenkov† and Heinz Frei*

Physical Biosciences Division, Mailstop Calvin Laboratory, Lawrence Berkeley National Laboratory, University of California, Berkeley, California 94720

Received: December 10, 1999; In Final Form: February 3, 2000

Step-scan FT-infrared spectroscopy of 1-naphthyl acetate and pinacolone photodissociation in zeolite NaY revealed a transient at 2125 cm^{-1} assigned to acetyl radical. Comparison of the intensities of transient and final product absorptions, 2-acetyl-1-naphthol in the case of naphthyl acetate and acetaldehyde for pinacolone, indicates that the acetyl radical represents the main, and probably only, reaction channel. The decay of the radical at room temperature is best described by a single-exponential law with a lifetime of 71 ± 15 μs (1-naphthyl acetate) and 315 ± 30 μs (pinacolone). This constitutes the first detection and kinetic study of a small transient radical in a zeolite. The kinetic result is interpreted in terms of complete separation of the photogenerated pairs from the parent supercage, followed by random walks in subspaces of the zeolite lattice imposed by the much less mobile precursor molecules. These force the geminate radicals to react and thereby contribute to the high selectivity of these photoreactions.

I. Introduction

Monitoring of transient radicals in zeolites and other microporous solids by time-resolved spectroscopy is essential for the mechanistic understanding of photochemical and catalytic reactions in these important materials. Aside from structural information on short-lived intermediates in microporous environments, elucidation of the kinetic behavior would reveal direct insight into the largely unknown factors that determine product selectivities and yields. Spectroscopy of transients in zeolites on the nano- and microsecond time scale has thus far been conducted exclusively on aromatic radicals and radical ions by UV−vis diffuse reflectance[1−10] and resonance Raman methods.[11,12] Optical transitions of small species that lack aromatic moieties are at too short wavelengths for monitoring inside zeolites by optical or resonance Raman spectroscopies. Therefore, these methods cannot be employed. Small transient species are key to much of the chemistry involved in the synthesis of everyday chemicals and fuels, an area where microporous materials play an increasing role.[13]

We have recently reported the first observation of a small transient radical in a zeolite by any technique, namely CH_3CO in NaY.[14] The technique employed was step-scan FT-infrared spectroscopy, which takes advantage of the infrared transparency of zeolites (above 1250 cm^{-1}) and the broad band nature of the FT method. The latter is particularly crucial when attempting to detect open-shell species in zeolites as infrared absorption frequencies may undergo large shifts that are difficult to predict. While step-scan FT-IR spectroscopy on the nanosecond and microsecond time scale is typically thought to be applicable only to reversible systems, or irreversible reactions under flowing sample conditions, we have demonstrated that the method can also be used for monitoring of irreversible reactions in static samples (a flow system that would replace samples between photolysis pulses is not practical in the case of zeolites).

In this paper, we communicate a full report on time-resolved FT-IR spectroscopy of acetyl radical generated by photodissociation of pinacolone and 1-naphthyl acetate precursor in zeolite NaY (Scheme 1). Kinetic data will be presented which indicate that the fate of the transient radicals in zeolites is very different from that in homogeneous solution. We find that it is strongly influenced by the presence of precursor molecules, an effect first established by Turro and co-workers, based on product analysis of static photolysis experiments.[15−17]

SCHEME 1

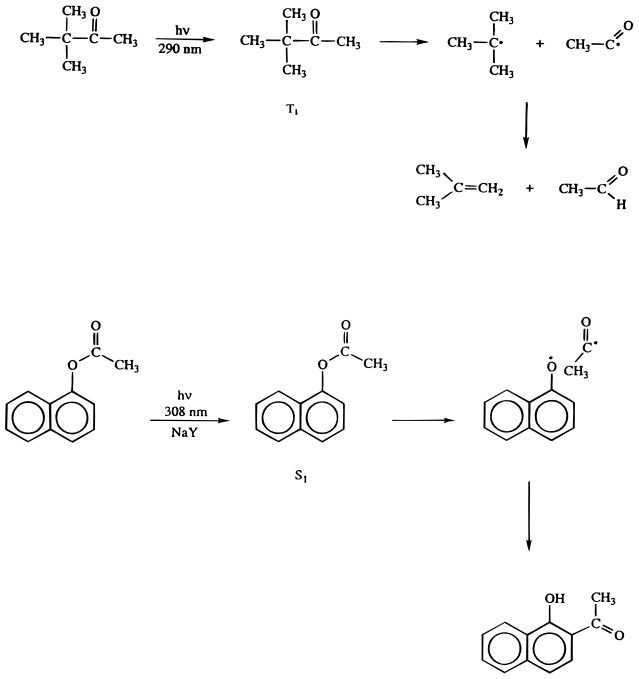

II. Experimental Section

For time-resolved FT-IR measurements a step-scan spectrometer, Bruker model IFS88, was used. This instrument was described in detail in a previous report.[18] Detectors used for

† Present address: Fakultät für Physik und Geowissenschaften, Universität Leipzig, Linnestrasse 5, D-04103 Leipzig, Germany.

10.1021/jp994366d CCC: $19.00
Published on Web 04/14/2000

experiments in the 2400−1900 cm^{-1} region were InSb PV detectors EG&G Judson model J100 (fwhm = 50 ns, RC decay of the AC-coupled preamplifer = 300 μs) and Kolmar Technologies model KISDP-1-J2 (fwhm = 48 ns, RC decay of AC-coupled preamplifier = 3.5 ms). For spectroscopy in the region 2000−1200 cm^{-1}, either an HgCdTe PV detector Kolmar Technologies model KMPV11-1-J2 (fwhm = 70 ns, RC decay of AC preamplifier = 3 ms) or an HgCdTe PV detector KMPV8-1-J2 (fwhm = 37 ns, RC decay of AC preamplifier = 1.4 ms) were employed. The latter was used for spectroscopy in the 2400−1900 cm^{-1} region as well. In the case of nanosecond time scale experiments (sampling interval = 25 ns), ac-coupled and dc-coupled interferometric signals were simultaneously acquired by a 40 MHz 12 bit digitizer (model PAD 1232). For time resolution of microseconds (sampling interval = 5 μs), a 200 kHz 16-bit digitizer was employed. Since no simultaneous processing capability for ac- and dc-coupled signals is available for this digitizer, a dc-coupled step-scan run of the sample (without excitation) was conducted first in order to obtain a phase spectrum. The stored phase spectrum was then used for phase correction of the ac-coupled interferogram time slices that were measure in the subsequent photolysis experiment. Time-resolved absorbance difference spectra were computed as

$$\Delta A = -\log\left(\frac{S + \Delta S}{S}\right)$$

where S stands for static single beam spectrum (Fourier transform of the dc-coupled interferogram) and ΔS the laser-induced spectrum (Fourier transform of the ac-coupled interferogram normalized for amplification).[18]

Samples were photolyzed with 8 ns pulses of a Quanta Ray model PDL-1 dye laser pumped by an Nd:YAG laser model DCR2A (GCR-3 optics). The pulse repetition rate was 10 Hz. 308 nm pulses (6 mJ $pulse^{-1}$) were generated by the second harmonic output of the dye Sulforhodamine 640, while 290 nm pulses (6 m J $pulse^{-1}$) were obtained by doubling the Kiton Red dye output. Photolysis light was aligned collinearly with the infrared probe beam by a small (1 cm edge-to-edge) prism. To prevent scattered photolysis light from reaching interferometer and detector optics, AR-coated Ge plates (International Scientific, 95% transmittance) were placed in the openings of the interferometer and detector compartments. Data acquisition was triggered by a small fraction of the photolysis laser pulse detected by an EG&G Silicon photodiode model SGD-444.

Folding limits for measurements with InSb detectors and HgCdTe detector model KMPV8-1-J2 were 2494 and 1663 cm^{-1} or 2430 and 1823 cm^{-1}, depending on whether the infrared filter W05200-6 or W04684-4 (Optical Coating Laboratory) was used. For spectroscopy in the fingerprint region, an OCLI filter model W07100-11X and folding limits 2106 and 1053 cm^{-1} were used. Filters were installed in front of the infrared detector. Spectral resolution was 4 cm^{-1}, resulting in step-scan runs of 420 mirror positions (2494−1663 cm^{-1}), 307 mirror positions (2430−1823 cm^{-1}), or 532 positions (2106−1053 cm^{-1}). At each mirror position, 15 laser-induced decays were recorded and averaged.

Self-supporting wafers of 6−8 mg of zeolite NaY (Aldrich, LZ-Y52, lot no. 12929CN) were pressed and placed inside a miniature infrared vacuum cell.[19] The infrared cell was mounted inside a variable temperature cryostat (Oxford model DN1724). The zeolite pellet was dehydrated at 473 K under high vacuum for 12 h (Varian turbomolecular pump model V-70), and pinacolone (Aldrich, 98%) loaded into the zeolite pellet from the gas phase after purification by trap-to-trap distillation. Loading levels were about 2 pinacolone molecules per supercage. Adsorption of 1-naphthyl acetate (Aldrich, 98%) into the zeolite NaY pores was achieved by stirring the zeolite powder in a hexane solution of 5 mg/mL ester at room temperature for 3 h. The zeolite was dehydrated prior to this loading procedure. The loaded zeolite was washed with excess hexane and evacuated for 12 h, and the resulting powder was pressed into wafers. Final dehydration of the pellets was conducted at ambient temperature under high vacuum, overnight.

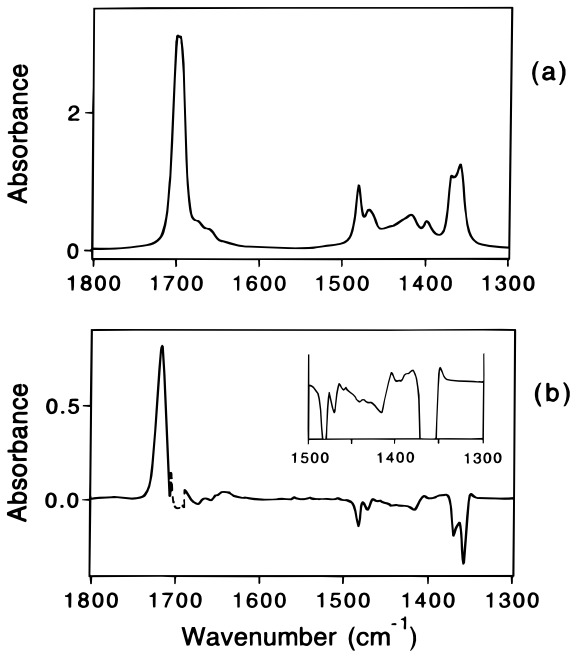

Figure 1. (a) Infrared difference spectrum upon loading of pinacolone into NaY from the gas phase. (b) Difference spectrum following 30 min irradiation of the matrix with 290 nm light at 6 mJ $pulse^{-1}$ (10 Hz). Inset shows the 1500−1300 cm^{-1} range on an expanded absorbance scale.

^{13}C-labeled 1-naphthyl acetate (carbonyl carbon) was prepared by adding acetic anhydride (1,1′-$^{13}C_2$) (Cambridge Isotope Laboratories, 99%) to a dilute solution of 1-naphthol (Aldrich, 98%) in aqueous caustic alkali.[20] The product was purified by repeated recrystallization from aqueous ethanol and dried in a vacuum. For spectroscopy of authentic samples of products, acetaldehyde (Aldrich, 99%), isobutene (Matheson, 99%), and 2-acetyl-1-naphthol (Aldrich, 98%) were used as received.

III. Results

1. Photodissociation of Pinacolone. An FT-IR spectrum of zeolite NaY loaded with pinacolone shows a very intense C=O stretch at 1697 cm^{-1} and weaker peaks at 1479, 1467, 1417, 1397, 1371, and 1359 cm^{-1} in the fingerprint region, and at 2977, 2929, 2915, and 2875 cm^{-1} in the C−H stretching region. Figure 1a gives the spectrum in the 1800−1300 cm^{-1} range. When irradiating the pellet at 290 nm (6mJ $pulse^{-1}$, 10 Hz) for 30 min, these bands decreased under concurrent growth at 2768, 1721, 1403, and 1348 cm^{-1}, as well as 1641, 1465, and 1381 cm^{-1}. The corresponding difference spectrum is shown in Figure 1b. These two groups of product bands are assigned to acetaldehyde and isobutene, respectively, based on comparison with infrared spectra of authentic samples in NaY. No other product growth was observed.

Step-scan FT-IR spectroscopy using 290 nm photolysis pulses of 8 ns duration revealed a transient at 2125 cm^{-1}, as reported

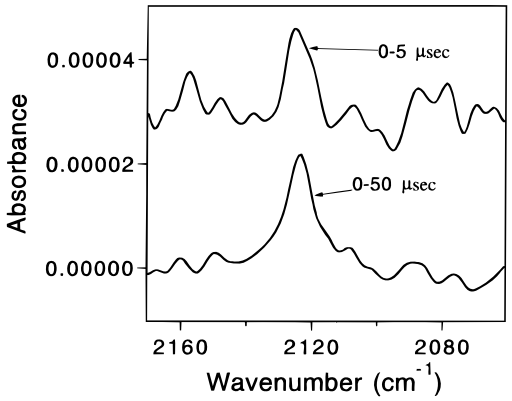

Figure 2. Step-scan FT-IR spectra of pinacolone photodissociation initiated by 290 nm laser pulses of 8 ns duration. Top trace: 5 μs time average obtained by coaddition of 200 time slices at 25 ns intervals. Bottom trace: 50 μs average recorded by coaddition of 10 time slices at 5 μs intervals. Details of measurements are described in the text.

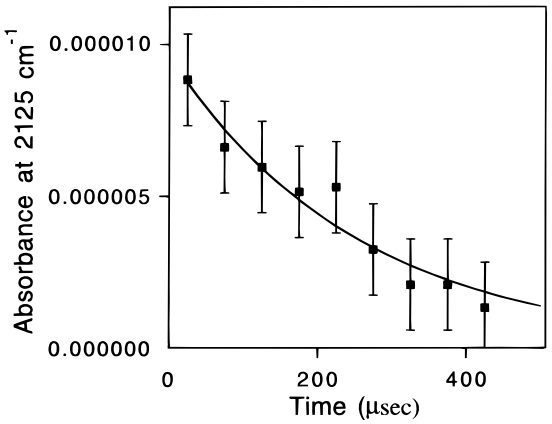

Figure 3. Decay of the 2125 cm^{-1} transient following photodissociation of pinacolone in NaY at 295 K. The solid curve represents a fit to a single-exponential law.

in our preliminary communication.[14] The top trace of Figure 2 shows the result of coaddition of 200 time slices taken at 25 ns intervals with a 40 MHz digitizer. 112 step-scan runs were averaged to obtain this spectrum. The bottom trace of Figure 2 was recorded with 5 μs sampling intervals and constitutes a time average over 50 μs (coaddition of 10 5 μs time slices). The spectra of 80 step-scan runs were averaged in order to reach a peak-to-peak noise of about 3×10^{-6} absorbance units. Because of the large reservoir of precursors, reactant depletion per step-scan run was less than one percent, thus minimizing distortion of spectra due to the irreversible nature of the system. The decay of the transient absorption at 295 K is displayed in Figure 3. Peak absorbances were used as the fwhm remained constant within uncertainties. Error bars reflect the average peak-to-peak absorbance fluctuation in the vicinity of the 2125 cm^{-1} band. The solid curve corresponds to a single-exponential fit with a decay constant of 260 $\pm$ 25 μs. Taking into account the distortion of the decay by the 1.4 ms RC constant of the detector preamplifier, a deconvoluted value of 315 $\pm$ 30 μs is calculated.[21] The decay was also measured at 245 K, and a lifetime of 500 $\pm$ 70 μs was observed.

Time-resolved FT-IR spectra recorded in the 2000−1700 cm^{-1} region, which encompasses the C═O stretch absorption of solution phase[22] or matrix-isolated[23] acetyl radical, did not reveal any transient. The HgCdTe detector required for these experiments is less sensitive than the InSb detector used for recording the 2125 cm^{-1} signal. Comparison of noise levels

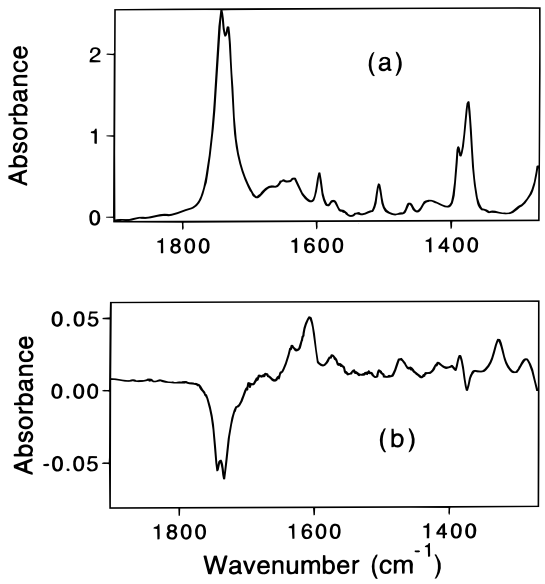

Figure 4. (a) Infrared difference spectrum upon loading of 1-naphthyl acetate into NaY. (b) Difference spectrum following 10 min photolysis at 290 nm (6 mJ pulse^{-1}, 10 Hz).

indicates that any band in the 2000−1770 cm^{-1} region that is twice as intense as the 2125 cm^{-1} absorption could have been detected.

2. Photodissociation of 1-Naphthyl Acetate. Zeolite NaY loaded with 1-naphthyl acetate showed infrared peaks at 1739, 1642, 1597, 1508, 1463, 1432, 1390, and 1377 cm^{-1} (Figure 4a). The static FT-IR difference spectrum recorded upon 10 min photolysis at 308 nm (6 mJ pulse^{-1}, 10 Hz), shown in Figure 4b, indicates product growth at 1637, 1605, 1573, 1504, 1469, 1386, 1327, and 1284 cm^{-1} under concurrent depletion of naphthyl acetate. Frequencies and intensities of the product bands agree with those of an authentic 2-acetyl-1-naphthol sample in NaY. No other product was detected.

Time-resolved FT-IR measurements of 1-naphthyl acetate photodissociation using 308 nm laser pulses again gave a transient absorption at 2125 cm^{-1}. Spectra and decay are shown in Figure 5. The sampling interval was 5 μs. Solid and dotted traces of Figure 5a correspond to coaddition of the first 10 (0−50 μs) and second 10 (50−100 μs) time slices, respectively. Spectra of 80 step-scan runs were averaged in the case of the parent ester. For observation of the transient upon ^{13}C naphthyl acetate dissociation (^{13}C labeled carbonyl group), which showed a 34 cm^{-1} red shift, 120 step-scan runs were averaged. The solid curve of Figure 5b represents the best fit to a single-exponential law with a lifetime of 60 $\pm$ 12 μs (raw data), or 71 $\pm$ 15 μs for the deconvoluted decay.

IV. Discussion

We will first discuss the spectroscopic identification of the intermediate. Then, a model will be proposed to explain the observed decay kinetics of the transient.

1. Assignment of the 2125 cm^{-1} Species. The ^{13}C isotope shift of 34 cm^{-1} agrees well with experimental and theoretical shifts of CO stretching modes of several acyl species, including acetyl radical isolated in a solid Ar matrix.[23] Equally, a 34 cm^{-1} ^{13}C shift of the 2130 cm^{-1} CO mode is observed for formyl cation in solution[24] and has also been predicted by ab initio calculations.[25] This frequency shift lies significantly below the 47 cm^{-1} value calculated in the harmonic approximation, which can be attributed to substantial anharmonicity of the CO mode.[25,26]

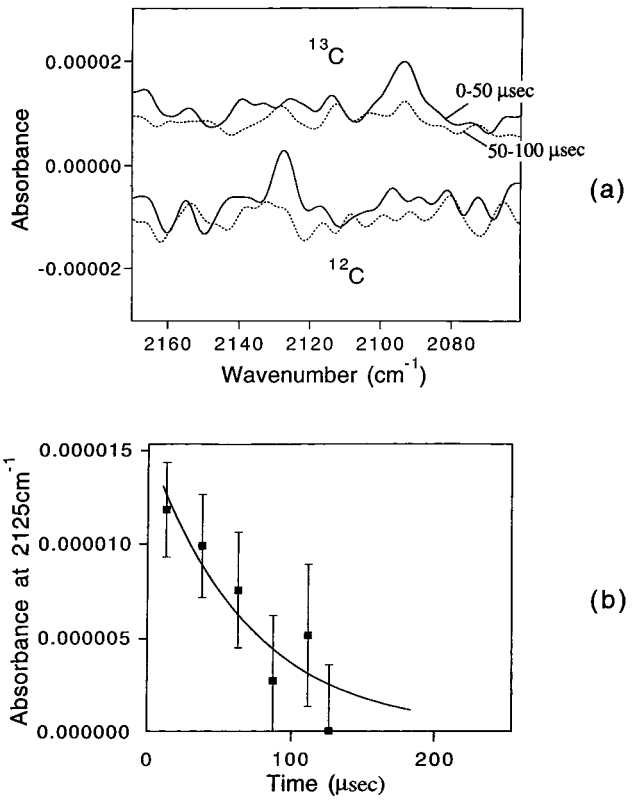

Figure 5. Step-scan FT-IR spectra of 1-naphthyl acetate photodissociation with 290 nm pulses of 8 ns duration. (a) Spectra taken at 5 μs sampling intervals, representing coaddition of 10 spectra over time ranges indicated. Spectra shown are baseline-corrected by subtracting a trace recorded after completion of the decay. ^{12}C, parent 1-naphthyl acetate precursor. ^{13}C, 1-naphthyl acetate with ^{13}C-labeled carbonyl group. (b) Kinetics of absorbance decay at 295 K. Error bars reflect average peak-to-peak noise in the vicinity of the band. The solid curve represents a fit to a single-exponential law.

While the isotope shift furnishes compelling evidence for a CH_3CO species, the large blue shift relative to the value for CH_3CO radical in hexane solution (1864 cm^{-1})[22] or solid Ar matrix (1875 and 1842 cm^{-1}, probably interacting with HF),[23] poses a question about its charge. Acyl cations are known to absorb in the 2100−2200 cm^{-1} region. For example, HCO^+ absorbs at 2184 cm^{-1} (gas phase)[27] or 2110 cm^{-1} (solution),[24] while CH_3CO^+ absorbs at 2200 cm^{-1} in solution.[28] However, formation of acetyl cation upon photodissociation of pinacolone is highly unlikely because there is no electron acceptor in this system that would make acetylium ion formation energetically feasible (*tert*-butyl radical is a poor electron acceptor).[29] On the other hand, it is well established that carbonyl species adsorbed onto cation-exchanged zeolites interact with the poorly shielded extraframework cations through the lone pair electrons on the O atom.[30,31] For closed-shell carbonyls, this results in a weakening of the CO double bond and, hence, a red shift of the stretching mode compared to the unperturbed molecule.

Molecular orbital considerations suggest an opposite effect for open-shell acyl species. The electronic structure of gas phase HCO radical (taken here as a model for unperturbed acetyl radical) features a singly occupied σ orbital on C(HOMO), σ-(CO) and π(CO) orbitals which constitute the CO double bond, and two O lone pair orbitals.[32,33] The CO stretch of isolated HCO radical lies at 1860 cm^{-1}.[34] As electron charge of the radical interacting in the zeolite is transferred from an O lone pair orbital toward Na^+, electron density is pulled from the singly occupied carbon σ orbital into the O lone pair σ orbital. As a result, interaction of these two HCO molecular orbitals leads to a more stable electron configuration with a substantial increase of the CO bond order beyond 2. This electron configuration is energetically not accessible in the absence of interaction with a cation. Hence, the formyl (acetyl) radical interacting with Na^+ is expected to have a CO stretching frequency close to that of HCO^+ with its triple bond absorbing at 2184 cm^{-1}, in agreement with the observed 2125 cm^{-1} transient (Figures 2 and 5). This explanation for the large blue shift in NaY is further supported by a recent ab initio study of the $HCO{\cdot}H_2O^+$ complex.[35] Interaction of the radical with hydronium ion was found to increase the CO stretching frequency by 216 cm^{-1}. Note, however, that the strong blue shift of CH_3CO does not necessarily imply a strong interaction of the radical with Na^+ ions. For example, in the case of NO_2, the asymmetric stretching mode is shifted to higher frequencies by several hundred cm^{-1} upon adsorption of the gas onto NaY, reflecting a change of the electron configuration closer to that of NO_2^+.[36] Yet, the species can easily be desorbed from the zeolite by evacuation at room temperature.[37]

Since we did not detect any transient infrared absorption around 1850 cm^{-1} where unperturbed CH_3CO radical would absorb,[22] it is likely that the 2125 cm^{-1} species is the only transient produced along the reaction path. In order to confirm this quantitatively, we compared the initial intensity of the 2125 cm^{-1} band (50 μs average) upon pinacolone photodissociation with that of the acetaldehyde growth at 1721 cm^{-1} per single laser pulse. Integrated intensities were determined as $(1.9 \pm 0.2) \times 10^{-4}$ cm^{-1} for acetyl radical and $(4.5 \pm 0.7) \times 10^{-4}$ cm^{-1} for the acetaldehyde absorption. Relative extinction coefficients of CH_3CO and CH_3CHO ν(CO) absorptions were assumed to be the same as the reported values for HCO radical and $CH_2{=}O$, with the coefficient of the aldehyde being twice that of the radical.[35,38] Hence, we calculate a concentration ratio CH_3CO/CH_3CHO of 0.90 ± 0.35. This estimate shows that, within uncertainties, CH_3CO radical interacting with Na^+ accounts for all acetyl species generated upon photodissociation.

2. Interpretation of Decay Kinetics. The decay of the acetyl radical signal in NaY is characterized by two features, namely, an unexpected long lifetime and the lack of second-order behavior. The nascent radical pair generated upon photolysis of 1-naphthyl acetate is a spin singlet since dissociation occurs mainly from the S_1 state of the ester (Scheme 1).[39] Therefore, if reaction of the geminate pair were to occur in the original supercage, it would most probably proceed within nanoseconds or faster. Pinacolone is known to dissociate from the triplet excited state.[40] There are precedents which indicate that, in a zeolite cage, spin flip required for geminate radical reactions is a nanosecond process.[2] Hence, the finding that CH_3CO survives for tens to hundreds of microseconds implies that the geminate radicals separate from the supercage in which they were generated and undergo random walks until they react. This process is facilitated by the availability of four large window openings for escape from the supercage.

Johnston et al. performed computer simulations of the decay of radical pairs in a NaX zeolite (isostructural with NaY) assuming random walk in an infinite lattice.[2] It was found that at a minimum half of the geminate radicals do not re-encounter. The nongeminate encounters of the radicals that would dominate the decay according to the computer simulations would follow a second-order reaction[2] described by eq 1 (ref 41), where R is the concentration of acetyl radical, k the bimolecular reaction rate constant, D the diffusion coefficient of acetyl radical in zeolite NaY, and ρ the reaction radius. The diffusion coefficient

$$R_t = \frac{R_0}{1 + ktR_0}$$

$$k = 8\pi D\rho \quad (1)$$

of acetyl radical is assumed to be the same as the measured value of propylene, 4×10^{-10} m^2 s^{-1}, which is of similar size and shape and has a similar degree of unsaturation.[42] This assumption is further supported by the activation energy of 1.7 kcal mol^{-1} derived by the Arrhenius law from the temperature dependence of the acetyl radical decay rates in the case of the pinacolone experiment. This activation energy is typical for diffusion of small alkenes in NaY.[43]

It is well established that, in the presence of much more abundant and less mobile aromatic coadsorbents such as naphthyl acetate, the diffusion coefficient of small, mobile species is reduced.[44] The diffusion coefficient of naphthyl acetate in the zeolite is about 4 orders of magnitude smaller than that of propylene.[43] Taking the known effect of coadsorbed benzene on the mobility of methane as a guide,[44] we estimate that in the presence of the precursor, the diffusion coefficient of acetyl radical is reduced by a factor of 10, to 4×10^{-11} m^2 s^{-1}. The supercage radius of 6 Å is taken as reaction radius,[45] and the initial acetyl radical concentration R_0 is calculated from measured infrared intensities as 4×10^{15} cm^{-3} (Figure 5a, corresponding to 56 pmol in the entire pellet). With these values, one obtains from eq 1 $R_t = 0.8R_0$ for $t = 100$ μs; i.e., the acetyl radical would decay by only 20% over the first 100 μs after the photolysis pulse. This is clearly not what is observed. According to Figure 5b, acetyl radical decays by 70% in the first 100 μs. Moreover, the long, distinct tail characteristic of a second-order decay is clearly lacking. In fact, as the solid traces in Figures 3 and 5b show, the decay of the 2125 cm^{-1} transient fits best a single-exponential law.

It is interesting to note that the kinetics of radical decay following 1-naphthyl acetate or pinacolone photodissociation in the zeolite differs from the corresponding reactions in homogeneous solution. UV−vis laser flash photolysis studies of the photo-Fries rearrangement revealed a transient absorbing of 385 nm, which was assigned to naphthoxy radical.[39,46] Laser-induced CIDNP experiments showed that the majority of the geminate naphthoxy and acetyl radicals react in the parent solvent cage, while 25% escape and give rise to a second-order decay due to nongeminate reaction on the 100 μs time scale. Similarly, in the case of CIDNP measurements of pinacolone photodissociation in solution, acetyl and *tert*-butyl radical are found to decay by a second-order rate law in the 10 μs time frame.[47]

The single-exponential behavior of the decay in the zeolite can be rationalized if one takes into account the effect of the precursor molecules on the intracrystalline diffusion path of the random hopping radicals. Our naphthyl acetate photolysis experiments were performed at a loading level of about one precursor per supercage on average. Since the diffusion coefficient of a substituted naphthalene molecule is about 4 orders of magnitude lower than the estimated acetyl radical coefficient, many supercage windows are "statically blocked."[44,48] In the case of such slowly diffusing molecules, a loading level of one per supercage implies that the system is well beyond the percolation threshold. The latter is defined as the minimum number of blockages required to prevent a random walking species to explore the entire volume of the zeolite crystallite, which corresponds to a loading of 0.5 molecules per supercage in this case.[44,48] Hence, the transient radicals are confined to subspaces of the zeolite particle, sometimes also referred to as pockets or bubbles.[15] A precedent for such behavior and the validity of percolation theory was established in a pulsed field gradient NMR study of a methane−benzene gas mixture in NaY by McCormick.[44] Benzene diffuses much more slowly ($D = 1 \times 10^{-11}$ m^2 s^{-1}) than methane ($D = 2 \times 10^{-8}$m^2 s^{-1}) in this zeolite. It was found that the only effect of C_6H_6 molecules was blocking of the diffusion path, leaving the jump rate and activation for diffusion of CH_4 essentially unchanged compared to the single-component CH_4−NaY system. Hence, the decreased diffusivity of methane in the presence of benzene is a percolation effect due to increased tortuosity of the diffusion path by blockage of passages. Naphthyl acetate and pinacolone precursor are expected to have an analogous effect on the much more mobile acetyl (or butyl) radicals, confining these to subspaces sufficiently small to prevent nongeminate encounters. Pinacolone may be more mobile than naphthyl acetate and, therefore, not as efficient a blocker. Higher loading levels are required in the case of partial blockage of zeolite cages,[48] which is fulfilled in our experiment as the pinacolone concentration is about 2 molecules per supercage.

The fate of a geminate radical pair in a finite subspace of zeolite Y is closely related to the problem of the survival of a random walker in a finite 3-dimensional lattice with a single trap. Analytical treatment of this problem reveals that the asymptotic decay of the survival probability is exponential with time, assuming that the initial position of the random walker with respect to the trap is random.[49,50] The average number of jumps required for a random walker in a 3-dimensional cubic lattice to be trapped is approximately 1.5 times the number of sites in the lattice.[51] Taking our estimated diffusion coefficient of acetyl radical and the center-to-center distance of 13 Å between supercages, the Einstein relation[52]

$$t = \frac{\langle r^2(t)\rangle}{6D} \quad (2)$$

gives a cage-to-cage hopping time of 0.7 ns. In the case of naphthyl acetate photodissociation, the lifetime of acetyl radical is 71 μs, which implies 1×10^5 jumps, or 6.7×10^4 cages probed by the radical. This corresponds to a volume of 1.2×10^8 Å^3, or a sphere of 300 Å radius. Because the calculation assumes unit quantum yield of reaction upon re-encounter of the geminate radicals in the same supercage, this radius is an upper limit and the pockets are probably smaller. From the concentration of acetyl radicals produced per laser pulse, 4×10^{15} cm^{-3}, we calculate an average separation of photolyzed naphthyl acetate or pinacolone molecules of 1300 Å. Hence, even in the case of unit quantum yield of radical reaction, the volumes explored by neighboring radical pairs would not intersect, thus preventing nongeminate encounters. If we take diffusion back and forth across the pocket as a criterion for randomization of the location of a radical, eq 2 allows us to conclude that this occurs within 3 μs after the photolysis pulse. This is even prior to taking the first data point of the decay curve and shows that the conditions for single-exponential decay of the random hopping radicals in the volumes confined by the precursor molecules are fulfilled. Differences in the mobility and loading of pinacolone and 1-naphthyl acetate in NaY, as well as in the mobility of *tert*-butyl and naphthoxy radical, may account for the different decay constant of acetyl radical for these two precursors. Our conclusion that photolysis of pinacolone or naphthyl acetate involves exclusively reaction of geminate radicals is also reflected in the complete selectivity and, especially, in the absence of radical self-coupling products.

Turro and co-workers were the first to present evidence for the effect of precursor molecules on the behavior of the more mobile radical photofragments in zeolites and rationalization in terms of percolation theory.[15−17] The main system used was dibenzyl ketone, and conclusions were based on final product distribution in static photolysis experiments. Using O_2 for scavenging of radicals in zeolite NaX, it was shown that, at high precursor loading, two-thirds of all geminate radical pairs escape the parent supercage and are forced to recombine in the subspace (secondary global cage)[16] imposed by the slowly moving precursor molecules.[17] This fraction was found to decrease dramatically with decreasing precursor loading, as the random hopping radicals find access to more and more expanding pockets.

V. Conclusions

Acetyl radical has been generated in zeolite NaY by photodissociation of 1-naphthyl acetate or pinacolone. The infrared spectrum reveals that interaction of the radical with the zeolite environment causes a change of the electronic structure of the radical toward a cation-like configuration. Unusually long lifetimes of acetyl radical from tens to hundreds of microseconds at room temperature indicate that the photogenerated radical pairs separate from the parent supercage. Single-exponential kinetics of the radical decay imply that products are formed by geminate radical encounters. This suggests that random walks of radicals are confined to subspaces of the zeolite crystallite that do not intersect with the ones occupied by neighboring radical pairs. These pockets are due to blockage by the much less mobile and many orders of magnitude more abundant precursor molecules. Hence, nongeminate encounters of transient radicals and, therefore, radical scrambling products are suppressed. This constitutes an important insight into the origin of selectivity of photochemical reactions in microporous solids.

More generally, this work establishes step-scan FT-IR spectroscopy as a tool for monitoring small transient radicals in zeolites. Specifically, we find that the technique can be applied to the important case of irreversible reactions in static samples. The broad band nature of the FT method is particularly useful for detecting radicals in zeolites as vibrational absorption frequencies may undergo large shifts in this environment that are difficult to predict. This spectroscopic tool is expected to lead to a new level of insight into the mechanism of reactions in microporous materials.

Acknowledgment. This work was supported by the Director, Office of Science, Office of Basic Energy Sciences, Chemical Sciences Division of the U.S. Department of Energy, under Contract No. DE-AC03-76SF00098.

References and Notes

(1) Kelly, G.; Willsher, C. J.; Wilkinson, F.; Netto-Ferreira, J. C.; Olea, A.; Weir, D.; Johnston, L. J.; Scaiano, J. C. *Can. J. Chem.* **1990**, *68*, 812.
(2) Johnston, L. J.; Scaiano, J. C.; Shi, J. L.; Siebrand, W.; Zerbetto, F. *J. Phys. Chem.* **1991**, *95*, 10018.
(3) Cozens, F. L.; Garcia, H.; Scaiano, J. C. *J. Am. Chem. Soc.* **1993**, *115*, 11134.
(4) Krueger, J. S.; Mayer, J. E.; Mallouk, T. E. *J. Am. Chem. Soc.* **1988**, *110*, 8232.
(5) Iu, K. K.; Thomas, J. K. *J. Phys. Chem.* **1991**, *95*, 506.
(6) Iu, K. K.; Thomas, J. K. *Colloids Surf.* **1992**, *63*, 39.
(7) Sankararaman, S.; Yoon, K. B.; Yabe, T.; Kochi, J. K. *J. Am. Chem. Soc.* **1991**, *113*, 1419.
(8) Yoon, K. B.; Hubig, S. M.; Kochi, J. K. *J. Phys. Chem.* **1994**, *98*, 3865.
(9) Gessner, F.; Scaiano, J. C. *Photochem. Photobiol. A: Chem.* **1992**, *67*, 91.
(10) Lednev, I. K.; Mathivanan, N.; Johnston, L. J. *J. Phys. Chem.* **1994**, *98*, 11444.
(11) Dutta, P. K.; Turbeville, W. *J. Phys. Chem.* **1992**, *96*, 9410.
(12) Maruszewski, K.; Strommen, D. P.; Kincaid, J. R. *J. Am. Chem. Soc.* **1993**, *115*, 8345.
(13) Hölderich, W. F.; van Bekkum, H. In *Introduction to Zeolite Science and Practice, Studies in Surface Science and Catalysis*; van Bekkum, H., Flanigen, E. M., Jansen, J. C., Eds.; Elsevier: Amsterdam, 1991; Vol. 58, p 631. (b) Sheldon, R. A.; Dakka, J. *Catal. Today* **1994**, *19*, 215. (c) Blatter, F.; Sun, H.; Vasenkov, S.; Frei, H. *Catal. Today* **1998**, *41*, 207.
(14) Vasenkov, S.; Frei, H. *J. Am. Chem. Soc.* **1998**, *120*, 4031.
(15) Turro, N. J.; Garcia-Garibay, M. A. In *Photochemistry in Organized and Constrained Media*; Ramamurthy, V., Ed.; VCH Publishers: New York, 1991; p 1.
(16) Garcia-Garibay, M. A.; Zhang, Z.; Turro, N. J. *J. Am. Chem. Soc.* **1991**, *113*, 6212.
(17) Garcia-Garibay, M. A.; Lei, X. G.; Turro, N. J. *J. Am. Chem. Soc.* **1992**, *114*, 2749.
(18) Sun, H.; Frei, H. *J. Phys. Chem. B* **1997**, *101*, 205.
(19) Blatter, F.; Frei, H. *J. Am Chem. Soc.* **1994**, *116*, 1812.
(20) Chattaway, F. *J. Chem. Soc.* **1931**, 2495.
(21) Demas, J. N. *Excited-State Lifetime Measurements*; Academic Press: New York, 1983.
(22) Brown, C. E.; Neville, A. G.; Rayner, D. M.; Ingold, K. U.; Lusztyk, J. *Aust. J. Chem.* **1995**, *48*, 365.
(23) Jacox, M. E. *Chem. Phys.* **1982**, *69*, 407.
(24) De Rege, P. J. F.; Gladysz, J. A.; Horvath, I. T. *Science* **1997**, *276*, 776.
(25) Puzzarini, C.; Tarroni, R.; Palmieri, P.; Carter, S.; Dore, L. *Mol. Phys.* **1996**, *87*, 879.
(26) Liu, P. J.; Lee, S. T.; Oka, T. *J. Mol. Spectrosc.* **1988**, *128*, 236.
(27) Foster, S. C.; McKellar, A. R. W.; Sears, T. J. *J. Chem. Phys.* **1984**, *81*, 578.
(28) Cook, D. *Can. J. Chem.* **1962**, *40*, 480.
(29) *Gas-Phase Ion Chemistry*; Bowers, M. T., Ed.; Academic Press: New York, 1979; Vol. 2.
(30) Geodakyan, K. T.; Kiselev, A. V.; Lygin, V. I. *Russ. J. Phys. Chem.* **1967**, *41*, 227.
(31) Howard, J.; Nicol, J. M. *J. Chem. Soc., Faraday Trans.* **1990**, *86*, 205.
(32) Adams, G. F.; Bent, G. D. *J. Chem. Phys.* **1979**, *71*, 3697.
(33) Yang, H. *Surf. Sci.* **1995**, *343*, 61.
(34) Ewing, G. E.; Thompson, W. E.; Pimentel, G. C. *J. Chem. Phys.* **1960**, *32*, 927.
(35) Coitino, E. L.; Pereira, A.; Ventura, O. N. *J. Chem. Phys.* **1995**, *102*, 2833.
(36) Chao, C. C.; Lunsford, J. H. *J. Am. Chem. Soc.* **1971**, *93*, 71.
(37) Kirkby, S. J.; Frei, H., to be submitted for publication.
(38) Galabov, B.; Bobadova, P.; Dudev, T. *J. Mol. Struct.* **1997**, *406*, 119.
(39) Gritsan, N. P.; Tsentalovich, Y. P.; Yurkovskaya, A. V.; Sagdeev, R. Z. *J. Phys. Chem.* **1996**, *100*, 4448.
(40) Vollenweider, J. K.; Fischer, H. *Chem. Phys.* **1988**, *124*, 333.
(41) Moore, J.; Pearson, K. *Kinetics and Mechanisms*, 3rd ed.; Wiley: New York, 1981; pp 19, 238.
(42) Hong, U.; Kärger, J.; Hunger, B.; Feoktistova, N. N.; Zhdanov, S. P. *J. Catal.* **1992**, *137*, 243.
(43) Kärger, J.; Ruthven, D. M. *Diffusion in Zeolites and Other Microporous Solids*; Wiley: New York, 1992; p 453.
(44) Nivarthi, S. S.; Davis, H. T.; McCormick, A. V. *Chem. Eng. Sci.* **1995**, *50*, 3217.
(45) Breck, D. W. *Zeolite Molecular Sieves: Structure, Chemistry, and Use*; Wiley: New York, 1974.
(46) Nakagaki, R.; Hiramatsu, M.; Watanabe, T.; Tamimoto, Y.; Nagakura, S. *J. Phys. Chem.* **1985**, *89*, 3222.
(47) Vollenweider, J. K.; Fischer, H.; Hennig, J.; Leuschner, R. *Chem. Phys.* **1985**, *97*, 217.
(48) Keffer, D.; McCormick, A. V.; Davis, H. T. *J. Phys. Chem.* **1996**, *100*, 967.
(49) Weiss, G. H.; Havlin, S.; Bunde, A. *J. Stat. Phys.* **1985**, *40*, 191.
(50) Den Hollander, W. T. F. *J. Stat. Phys.* **1985**, *40*, 201.
(51) Musho, M. K.; Kozak, J. J. *J. Chem. Phys.* **1984**, *81*, 3229.
(52) Kärger, J.; Ruthven, D. M. *Diffusion in Zeolites and Other Microporous Solids*; Wiley: New York, 1992; p 25.